A p-MUS Preconditioner for the EFIE

Michael Bluck, Nicolas Cinosi, and Simon Walker

***Abstract*—This paper considers the solution of the electric field integral equation (EFIE) in electromagnetics. As with associated finite element methods, their solution relies upon the construction of conforming bases. While lowest order (RWG) spaces are near ubiquitous, their extension to higher order offers, potentially, a number of benefits in terms of accuracy and efficiency, which has been well documented in both finite elements and integral equation formulations. A further evolution of higher order conforming bases is the hierarchical basis. These have demonstrated considerable gains in efficiency in finite element applications. Such bases allow for the development of effective acceleration schemes, for instance, the multilevel Schwarz type preconditioner (p-MUS). An obvious question arises as to the applicability of such hierarchical bases and their associated acceleration schemes to integral equations. It is seen that the conclusions as to their efficacy depend strongly on the scattering regime. In particular, high-frequency problems (those where the wavelength is the principal determinant of mesh size) are shown to benefit little from hierarchical functions. On the other hand, for "low-frequency" problems (where geometry is the main determinant of mesh size), there are significant improvements in performance over corresponding interpolatory schemes.**

***Index Terms*—Integral equation (IE), hierarchical, preconditioner.**

I. Introduction

THE solution of the integral equations, especially the electric field integral equation (EFIE), is notably challenging. Nonetheless, integral equation (IE) schemes have become a powerful tool, particularly with the development of accelerated schemes such as the fast multipole method (FMM) [1]. Key to most such treatments is the requirement to solve matrix equations iteratively, which at their core involve matrix-vector multiplications. Much of the cost of such solutions then depends on the number of iterations and the cost per iteration. There has been much work in reducing the number of iterations via the use of various preconditioners [2]–[5].

The vast majority of IE implementations (accelerated or otherwise) employ the simplest Rao–Wilton–Glisson (RWG) basis functions on triangles [6]. High order interpolatory bases have been developed which (in principle) offer improved accuracy for a given cost, though these are comparatively recent developments, such as [7].

The next natural step beyond high-order interpolatory methods is to arrange these bases hierarchically. Many variations on such hierarchical bases have been extensively studied within the finite element community [8]–[18], but little has been done for integral equations such as those studied here, though we should note [19], [20] and [21]. In [20], a two level scheme is demonstrated, employing a spectral preconditioning technique. More recently, classes of hierarchical conforming bases have been developed for a wide range of element types for both finite and integral equation methods [22]–[24]. Such bases are concisely described in terms of differential forms and it is this terminology which we adopt here, although this is essentially a notational convenience and the results apply to standard vector forms of bases. Of themselves hierarchical bases offer little more than their high order interpolatory counterparts. However, as has been demonstrated in finite elements [17], [18], [25], [26] it is possible to employ this hierarchical structure to great effect in the reduction of the computational cost of the underlying iterative scheme via a multilevel Schwarz type preconditioner (p-MUS). In this paper we will demonstrate the application of hierarchical bases to integral equations and investigate the efficiency gains (if any) to be achieved.

In Section II, we briefly recall the form of the EFIE and the hierarchical bases used in this work. These bases are detailed in [27]. In Section III, a p-MUS multilevel preconditioner is described, together with results demonstrating its effectiveness on selected problems. It is noted that there is limited (if any) gain for frequency dominated problems due to the existence of a critical level of discretization, below which, the p-MUS method fails to converge. Except in exceptional circumstances (those requiring very high accuracy), such methods offer little in terms of efficiency gains over conventional interpolatory bases. The key result presented here is that the principal benefits of the p-MUS approach lie in its application to problems where discretization is determined by geometrical complexity. In such cases, it is clear that a speed-up of between 5 and 20 times their conventional interpolatory counterparts are achieved. Such cases arise frequently in areas such as frequency selective surfaces (FSS), antenna arrays and sub-wavelength resolution.

II. Differential Forms and the EFIE

Using the notation of differential forms, a discretized Galerkin form of the EFIE on a surface S can be written as [22]

$$\frac{i}{kc}\int_S \omega_i \wedge E^{inc} = \int_S \omega_i \wedge \int_S gI \wedge \sum_j \omega_j h_j + \frac{1}{k^2}\int_S d'\omega_i \wedge \int_S g \sum_j d\omega_j h_j \quad (1)$$

where E^{inc} is an incident wave, k the wavenumber, g the free-space green function for the Helmholtz equation, ω_i the i^{th} basis function and h_i are the unknown surface magnetic field coefficients.

While the notation may be unfamiliar to many in the EM community, it has the advantage of explicitly separating the field approximation from the geometry description. This makes the implementation of curvilinear geometry modeling much more straightforward. The conventional vector notation using RWG type functions requires that the bases also embody geometric,

Manuscript received October 29, 2012; revised March 12, 2013, June 07, 2013; accepted July 30, 2013. Date of publication August 06, 2013; date of current version October 28, 2013.

The authors are with the Department of Mechanical Engineering, Imperial College, London, SW7 2AZ, U.K. (e-mail: m.bluck@imperial.ac.uk).

Digital Object Identifier 10.1109/TAP.2013.2276926

TABLE I
HIERARCHICAL BASES ON PARENT TRIANGLE

k	σ	Bases
1	$\sigma_{1,1}$	$(1-\zeta_2)\,d\zeta_1+\zeta_1 d\zeta_2$
	$\sigma_{1,2}$	$-\zeta_2 d\zeta_1+\zeta_1 d\zeta_2$
	$\sigma_{1,3}$	$-\zeta_2 d\zeta_1+(\zeta_1-1)\,d\zeta_2$
2	$\sigma_{1,1}$	$(2\zeta_1+\zeta_2-1)\,d\zeta_1+\zeta_1 d\zeta_2$
	$\sigma_{1,2}$	$-\zeta_2 d\zeta_1-\zeta_1 d\zeta_2$
	$\sigma_{1,3}$	$\zeta_2 d\zeta_1+(\zeta_1+2\zeta_2-1)\,d\zeta_2$
3	$\sigma_{1,1}$	$\left(4-24\zeta_1+24\zeta_1^2-7\zeta_2+21\zeta_1\zeta_2+3\zeta_2^2\right)d\zeta_1+$ $\left(-5\zeta_1+9\zeta_1^2+3\zeta_1\zeta_2\right)d\zeta_2$
	$\sigma_{1,2}$	$\left(2\zeta_2+6\zeta_1\zeta_2-6\zeta_2^2\right)d\zeta_1+\left(-2\zeta_1-6\zeta_1\zeta_2+6\zeta_2^2\right)d\zeta_2$
	$\sigma_{1,3}$	$\left(5\zeta_2-9\zeta_2^2-3\zeta_1\zeta_2\right)d\zeta_1+$ $\left(-4+7\zeta_1-3\zeta_1^2+24\zeta_2-21\zeta_1\zeta_2-24\zeta_2^2\right)d\zeta_2$
	$\sigma_{2,1}$	$\left(\zeta_2-2\zeta_1\zeta_2-\zeta_2^2\right)d\zeta_1+\left(\zeta_1-2\zeta_1\zeta_2-\zeta_1^2\right)d\zeta_2$ $\left(\zeta_2+2\zeta_1\zeta_2-\zeta_2^2\right)d\zeta_1+\left(5\zeta_1-5\zeta_1^2-2\zeta_1\zeta_2\right)d\zeta_2$ $\left(-33\zeta_2+27\zeta_1\zeta_2+33\zeta_2^2\right)d\zeta_1+$ $\left(21\zeta_1-21\zeta_1^2-27\zeta_1\zeta_2\right)d\zeta_2$

TABLE II
HIERARCHICAL BASES ON PARENT SQUARE

k	σ	Bases
1	$\sigma_{1,1}$	$(1-\zeta_2)\,d\zeta_1$
	$\sigma_{1,2}$	$\zeta_1 d\zeta_2$
	$\sigma_{1,3}$	$-\zeta_2 d\zeta_1$
	$\sigma_{1,4}$	$-(1-\zeta_1)\,d\zeta_2$
2	$\sigma_{1,1}$	$\frac{1}{4}(5\zeta_2-2)(\zeta_2-1)(2\zeta_1-1)\,d\zeta_1$
	$\sigma_{1,2}$	$\frac{1}{4}\zeta_1(2\zeta_2-1)(5\zeta_1-3)\,d\zeta_2$
	$\sigma_{1,3}$	$-\frac{1}{4}\zeta_2(5\zeta_2-3)(2\zeta_1-1)\,d\zeta_1$
	$\sigma_{1,4}$	$-\frac{1}{4}(5\zeta_1-2)(\zeta_1-1)(2\zeta_2-1)\,d\zeta_2$
	$\sigma_{2,1}$	$\zeta_2(\zeta_2-1)\,d\zeta_1$ $\frac{1}{2}\zeta_2(\zeta_2-1)(2\zeta_1-1)\,d\zeta_1$ $-\zeta_1(\zeta_1-1)\,d\zeta_2$ $-\frac{1}{2}\zeta_1(\zeta_1-1)(2\zeta_2-1)\,d\zeta_2$
3	$\sigma_{1,1}$	$\frac{1}{6}(1-\zeta_2)\left(7\zeta_2^2-6\zeta_2+1\right)\left(6\zeta_1^2-6\zeta_1+1\right)d\zeta_1$
	$\sigma_{1,2}$	$\frac{1}{6}\zeta_1\left(6\zeta_2^2-6\zeta_2+1\right)\left(7\zeta_1^2-8\zeta_1+2\right)d\zeta_2$
	$\sigma_{1,3}$	$-\frac{1}{6}\zeta_2\left(7\zeta_2^2-8\zeta_2+2\right)\left(6\zeta_1^2-6\zeta_1+1\right)d\zeta_1$
	$\sigma_{1,4}$	$-\frac{1}{6}(1-\zeta_1)\left(7\zeta_1^2-6\zeta_1+1\right)\left(6\zeta_2^2-6\zeta_2+1\right)d\zeta_2$
	$\sigma_{2,1}$	$\frac{1}{6}\zeta_2\left(6\zeta_1^2-6\zeta_1+1\right)(\zeta_2-1)\,d\zeta_1$ $\frac{1}{12}\zeta_2(2\zeta_2-1)(\zeta_2-1)\left(6\zeta_1^2-6\zeta_1+1\right)d\zeta_1$ $\frac{1}{4}\zeta_2(2\zeta_2-1)(\zeta_2-1)(2\zeta_1-1)\,d\zeta_1$ $\frac{1}{2}\zeta_2(2\zeta_2-1)(\zeta_2-1)\,d\zeta_1$ $\frac{1}{6}\zeta_1\left(6\zeta_2^2-6\zeta_2+1\right)(\zeta_2-1)\,d\zeta_2$ $\frac{1}{2}\zeta_1(2\zeta_1-1)(\zeta_1-1)\,d\zeta_2$ $\frac{1}{4}\zeta_1(2\zeta_1-1)(\zeta_1-1)(2\zeta_2-1)\,d\zeta_2$ $\frac{1}{12}\zeta_1(2\zeta_1-1)(\zeta_1-1)\left(6\zeta_2^2-6\zeta_2+1\right)d\zeta_2$

as well as field information. In fact, RWG type bases can be obtained as Hodge star operations (corresponding to a cross product with a unit normal; a 90 degree rotation) on these 1-form bases, as shown in [22].

Given this, it remains to specify precisely the discretization of these equations, and three choices must be made. First, the geometry: In this implementation, we describe the geometry using six noded Lagrangian triangular elements and/or nine noded quadratic square elements. Second, the surface fields must be approximated by basis functions: We will choose a class of hierarchical conforming basis functions (shown in Tables I and II up to third order) obtained as surface traces of the functions developed in [27]. These have been shown to be well-conditioned in a finite element sense. Third, we will employ a Galerkin approach and must specify appropriate testing functions: We will choose the very same bases used to approximate the fields, as is the norm with such formulations.

III. P-MUS GAUSS-SEIDEL MULTILEVEL PRECONDITIONING

Such hierarchical bases can be shown to be highly effective, certainly in finite element formulations. An attractive approach is the a multiplicative Schwarz method. To explain this, consider a problem for which $k=1$. Solving the IE for this case gives rise to a matrix equation $A_{11}\mathbf{x}_1=\mathbf{b}_1$. Now consider the case for $k=2$. In principle, we may form the entire matrix

$$\begin{bmatrix} A_{11} & A_{12} \\ A_{21} & A_{22} \end{bmatrix}\begin{bmatrix} \mathbf{x}_1 \\ \mathbf{x}_2 \end{bmatrix}=\begin{bmatrix} \mathbf{b}_1 \\ \mathbf{b}_2 \end{bmatrix}. \tag{2}$$

Note that the first diagonal block of A and the first block of $\mathbf{b}$ is unchanged from the first-order case. We may attempt a full solution of this, treating the $k=2$ case as an entirely new problem (we term this a single level (SL) scheme). Rather, as is the case with some hierarchical FE implementations, we use the result of the $k=1$ calculation to aid us in the solution of the second order problem, and so on, in principle to arbitrary degree (we term this a Multilevel (ML) scheme). In the scheme proposed here, we employ a block Gauss–Siedel method. For the $k=2$ case above, we begin by obtaining a solution $\mathbf{x}_1$ to the $k=1$ case, that is, we solve

$$[A_{11}][\mathbf{x}_1]=[\mathbf{b}_1]. \tag{3}$$

We then use this result to compute $\mathbf{x}_2$ via

$$[A_{22}][\mathbf{x}_2]=[\mathbf{b}_2]-[A_{21}][\mathbf{x}_1]. \tag{4}$$

We can now return to the first-order problem, with a perturbed RHS and compute a new $\mathbf{x}_1$, i.e.,

$$[A_{11}][\mathbf{x}_1]=[\mathbf{b}_1]-[A_{12}][\mathbf{x}_2]. \tag{5}$$

We proceed by repeating this cycle, successively solving (4) and (5) until convergence is achieved.

The solutions of the individual block matrix equations [(4) and (5)] can be performed with any appropriate solver and in this work we have used a complex bi-conjugate gradient algorithm (BiCG).

This procedure generalizes to arbitrary order, and is embodied in the following algorithm:

while $\epsilon > TOL$ **do**
  for $i=1$ to p **do**
    $\mathbf{c}_i=\mathbf{b}_i$
    for $j=1$ to p, $j\neq i$ **do**
      $\mathbf{c}_i=\mathbf{c}_i-A_{ij}\mathbf{x}_j$
    end for
    $\{\mathbf{x}_i,\epsilon_i\}=BiCG\{A_{ii},\mathbf{c}_i,TOL_i\}$
  end for
  for $i=p-1$ to 2 **do**
    $\mathbf{c}_i=\mathbf{b}_i$
    for $j=1$ to p, $j\neq i$ **do**
      $\mathbf{c}_i=\mathbf{c}_i-A_{ij}\mathbf{x}_j$
    end for
    $\{\mathbf{x}_i,\epsilon_i\}=BiCG\{A_{ii},\mathbf{c}_i,TOL_i\}$
  end for
end while

where $\mathbf{x}_i$ denotes the coefficient vector of order i. The convergence criteria for the solution of all matrix equations is that

$$\epsilon = \frac{\|\mathbf{b} - A\mathbf{x}\|_2}{\|\mathbf{b}\|_2} < TOL \tag{6}$$

with analogous expressions for the subproblems. The tolerances are denoted by *TOL* for the overall problem and TOL_i for the subproblems. Note that this is a classical V-cycle in multigrid terminology.

A. Convergence of the p-MUS Scheme

The assumption has been made that the p-MUS scheme converges. As we shall see, this is not always the case (even if each sub matrix solution does) and it is worthwhile considering why this may be the case. We begin by considering the residual obtained at the end of each cycle, for the $k = 2$ case. If we recast the equations in terms of successive corrections and we have an approximate solution $\tilde{\mathbf{x}}$ after the ith cycle, given by

$$\tilde{\mathbf{x}} = \begin{bmatrix} \tilde{\mathbf{x}}_1 \\ \tilde{\mathbf{x}}_2 \end{bmatrix}. \tag{7}$$

With analogous notation for other vectors. The ith residual at this cycle is clearly

$$\tilde{\mathbf{r}}^i = \tilde{\mathbf{b}} - A\tilde{\mathbf{x}} \tag{8}$$

where A is the full matrix. At the next cycle $(i+1)$, we obtain a new solution $\mathbf{x}$, which we can express as a correction $\mathbf{x}^1$ to the old solution, that is we let

$$\mathbf{x} = \tilde{\mathbf{x}} + \mathbf{x}^1. \tag{9}$$

Or equivalently that $\mathbf{x}^1$ is the solution to

$$A\mathbf{x}^1 = \tilde{\mathbf{r}}^i. \tag{10}$$

The Gauss–Seidel cycle obtains the correction as

$$\mathbf{x}^1 = \begin{bmatrix} \mathbf{x}_1^1 \\ \mathbf{x}_2^1 \end{bmatrix} = \begin{bmatrix} A_{11}^{-1}\mathbf{r}_1^i \\ A_{22}^{-1}\left(\mathbf{r}_2^i - A_{21}\mathbf{x}_1^1\right) \end{bmatrix} \tag{11}$$

which can be written explicitly as

$$\mathbf{x}^1 = \begin{bmatrix} A_{11}^{-1}\mathbf{r}_1^i \\ A_{22}^{-1}\left(\mathbf{r}_2^i - A_{21}A_{11}^{-1}\mathbf{r}_1^i\right) \end{bmatrix}. \tag{12}$$

It is then clear that

$$\begin{aligned} \tilde{\mathbf{r}}^{i+1} &= \tilde{\mathbf{b}} - A\mathbf{x} \\ &= \tilde{\mathbf{b}} - A\tilde{\mathbf{x}} - A\mathbf{x}^1 \\ &= \tilde{\mathbf{r}}^i - A\mathbf{x}^1. \end{aligned} \tag{13}$$

Combining (12) and (13) we obtain

$$\tilde{\mathbf{r}}^{i+1} = C\tilde{\mathbf{r}}^i \tag{14}$$

where

$$C = \begin{bmatrix} A_{12}A_{22}^{-1}A_{21}A_{11}^{-1} & -A_{12}A_{22}^{-1} \\ 0 & 0 \end{bmatrix}. \tag{15}$$

Clearly, if the eigenvalues of the matrix C lie within the unit disc then the scheme will converge. Note that this discussion assumes exact inversion of the sub-matrices, which gives rise to the zero entries in the second row of C (and associated zero eigenvalues). In practice, the BiCG is used for the sub-matrix equation solution, with a large tolerance, so in reality we have an approximate inverse and these entries will generally differ somewhat from zero. Nevertheless, convergence will likely be determined by the largest eigenvalue of the matrix in the first entry of C. We will demonstrate this link between the spectrum of the iteration matrix C and convergence of the p-MUS scheme in the following section.

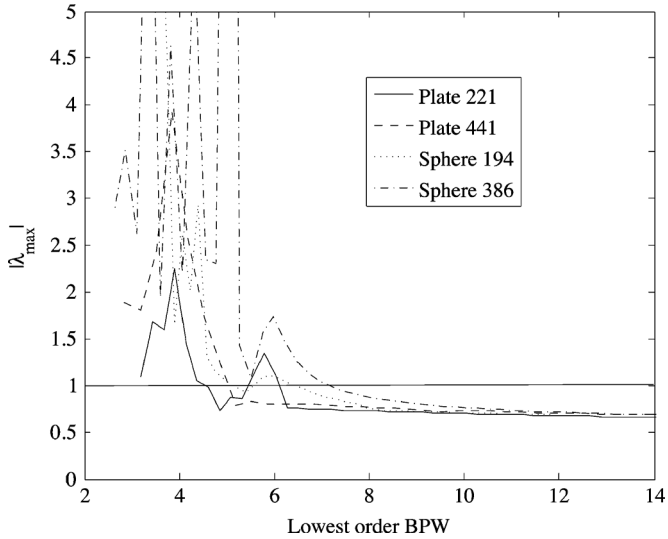

Fig. 1. Modulus of largest eigenvalue of C for plates (221 and 441 nodes) and spheres (194 and 386 nodes) versus Number of bases per wavelength at lowest order.

B. Results

The multilevel scheme (ML) developed in the previous section is applied to a range of canonical problems including spheres, plates, cubes, and dihedrals. In each case, we also compute the computational cost based on both a non-accelerated scheme (where each iteration involves $O(N^2)$) operations) and an accelerated scheme (e.g., where each iteration involves $O(NlogN)$ operations). In these cases $TOL = 10^{-5}$ and $TOL_i = 10^{-5}$. These costs are compared with a direct application of the BiCG method (a single level scheme (SL)) to the "entire" matrix, again with $TOL = 10^{-5}$.

We begin by investigating the convergence properties of the p-MUS scheme. Numerical experiments demonstrate the importance of an appropriate degree of mesh refinement: If the number of bases per linear wavelength (BPW) for the lowest order is less than $\sim$7, the ML scheme is prone to divergence. The relationship between convergence and discretization is demonstrated clearly in Fig. 1, where the modulus of the largest eigenvalue, $\lambda_{\max}$, of the matrix C is plotted against the lowest order BPW for two plate and sphere cases in a 2-level p-MUS scheme. These results are obtained by varying the incident wavelength and mesh refinement in each case. Note that in all cases where $|\lambda_{\max}| < 1$ we obtain convergence and that beyond some critical value of lowest order BPW this is always the case. Note that given this baseline discretization ($\sim$7 *BPW*), a 2-level problem will have $\sim$11 *BPW* and a 3-level problem $\sim$14 *BPW*. It is clear that it is necessary to have a "good enough" lowest order approximation.

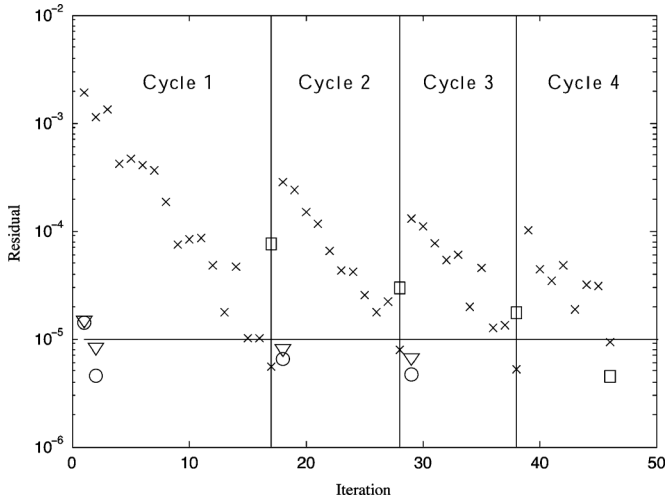

Fig. 2. Residual versus iteration for a PEC cube (350 DoF): (×)—level 1, (○)—level 2, (▽)—level 3, (□)—total residual.

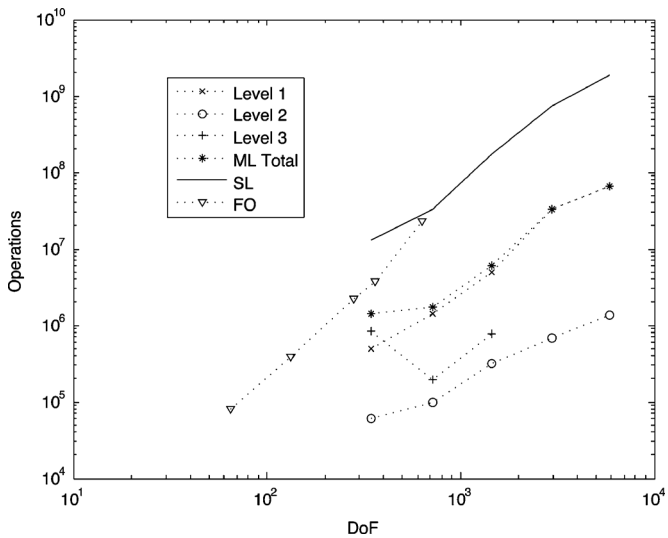

Fig. 3. Operation count for multilevel scheme, single-level scheme, and first-order only scheme—flat PEC plate.

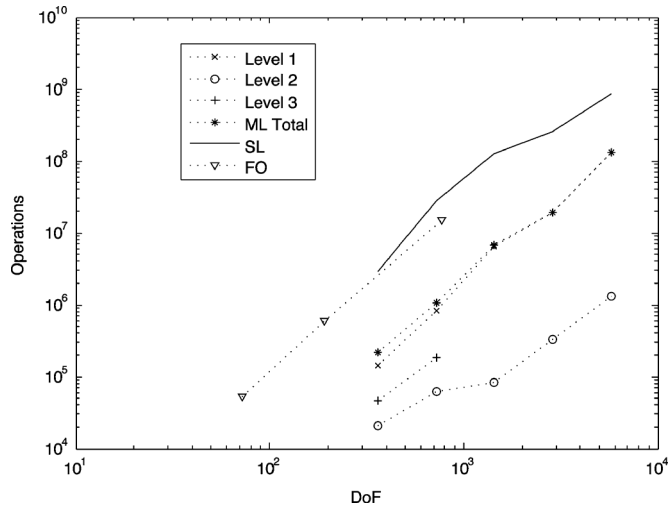

Fig. 4. Operation count for multilevel scheme, single-level scheme, and first-order only scheme—PEC sphere.

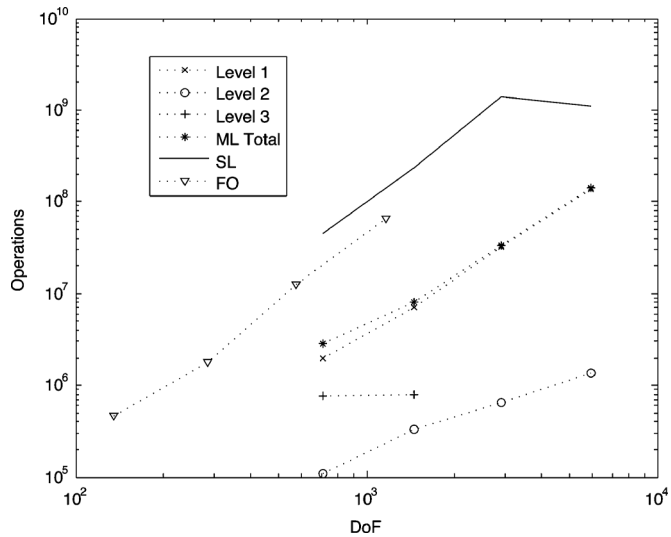

Fig. 5. Operation count for multilevel scheme, single-level scheme, and first-order only scheme—PEC dihedral.

It is clear from Fig. 1 that in the limit of very fine meshes, $|\lambda_{\max}|$ tends to a fixed value (~ 0.7), independent of the geometry. Also from Fig. 1, we see that the baseline BPW is weakly dependent on the geometry. In particular, the dihedral (not shown in the figure) is more demanding than the other shapes, requiring a lowest order BPW of $\sim$8 for convergence. This is possibly due to the higher Q of the dihedral, although this is little more than speculation. In the following examples, in order to make appropriate comparisons, we fix the number of overall bases in a 3-level scheme at roughly 15 BPW (except for the dihedral case, where we choose $BPW = 17$). Thus, we increase the number of bases by refining the mesh, as we increase frequency. This, then, allows us to approximately fix the discretization error.

The BiCG residuals are plotted against cumulative iteration number in Fig. 2 for a 350 DoF PEC cube. It is clear that most iterations occur for the lowest order (level 1) and that convergence is very rapid for levels 2 and 3. The operation count is plotted as a function of number of degrees of freedom in Figs. 3–5 for plates, spheres, and dihedrals, respectively. These problems range from approximately 1λ to 5λ in size. It is clear from these cases that the majority of the computational cost is in the lowest order calculation (Level 1), with significantly fewer iterations required for the high-order cases (Level 2 & 3). Indeed, the higher level iterations have frequently converged after just one or two iterations. Given the lowest order baseline required for convergence, there seems little point in going beyond the third order. This is probably due to the fact that 15 BPW (or 17 in the dihedral case) is enough to capture all of the scattering processes. This may not, of course, always be the case and there may be circumstances when higher level schemes are beneficial, as we shall note later. These figures also include the cost for a conventional "single level—third order" (SL) application of the BiCG, (i.e., simply applying the BiCG to the whole impedance matrix) and the cost for a conventional first-order (FO) RWG type calculation. Comparing the SL result with the FO result appears to indicate that there is little benefit to be had in the use of high-order basis functions in isolation. However, this is misleading—one would reasonably expect that for a given accuracy

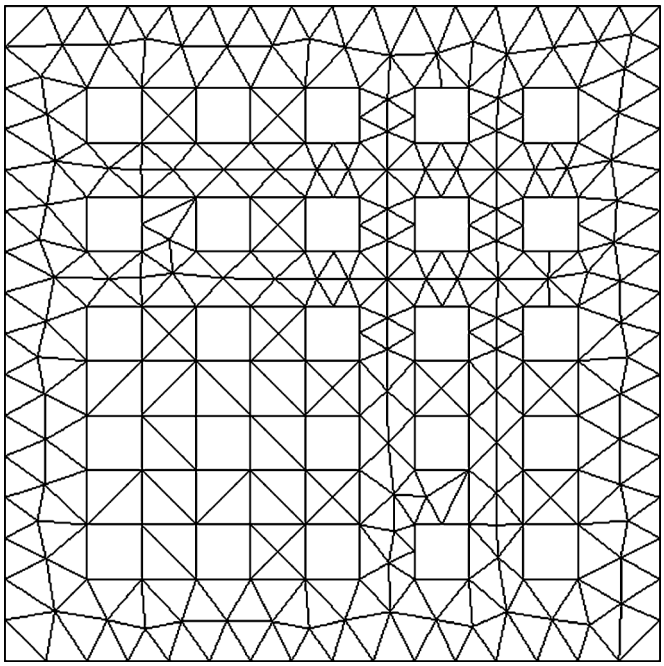

Fig. 6. Aperture array Mesh with 475 triangular elements.

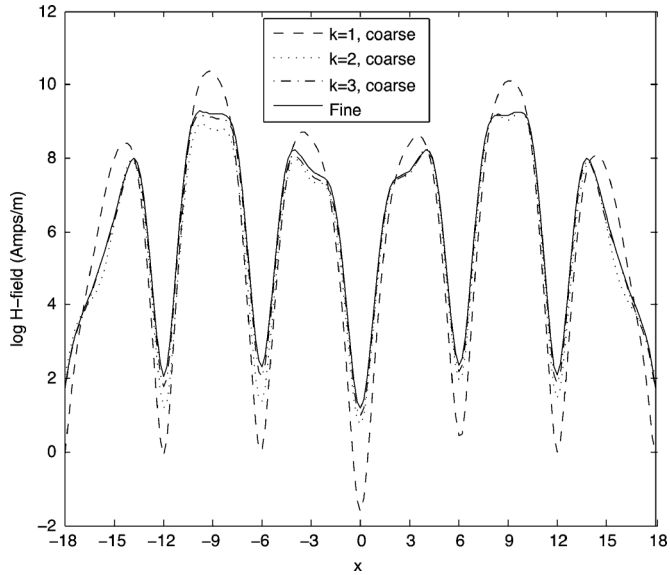

Fig. 7. H-field near aperture array versus position across the plate along a line through the midsection.

of result we could employ significantly fewer high-order bases than the conventional first-order case.

We see from these figures that the computational cost of the ML scheme in comparison with the conventional application of the BiCG to the overall matrix equation results in a speed-up by up to a factor ~ 20. Note also that the effective cost for an accelerated (e.g., FMM) scheme results in a speed-up by a factor ~ 5.

While these results appear promising, they do obscure an underlying problem. The critical value places a lower bound on the discretization. In fact, used as a single level scheme, third-order bases can deliver sufficient accuracy (for far field scattering) for ~ 5 BPW, which corresponds to a lowest order discretization of ~ 3 BPW. Note that the multilevel scheme would simply not converge in such circumstances. In the comparisons shown, we have used a discretization of 15 BPW at third order. In applications where the discretization is determined principally by the frequency (e.g., large smooth antennas and canonical RCS problems), it is clear that there is little gain (if any) to be had in using hierarchical bases in this fashion. However, a large and growing body of cases arise where the discretization is determined by geometry, notably frequency selective surfaces, sub-wavelength resolution and sub-wavelength waveguides, etc. By their very nature, feature size in such cases is less than a wavelength, although the overall target size could still be large. It is necessary to resolve these features properly to accurately predict resonances, transmission coefficients and the like. For these cases, the wavelength is relatively large in comparison with the feature size and many of these problems result in discretizations of ~ 15 BPW and more, as a by product of the requirement to model the geometry accurately. In such cases the gains made by the p-MUS approach would be realized.

An example of such a problem is given next: This involves a plate with square apertures, of the kind arising in metamaterials and sub-wavelength resolution problems. The apertures are sub-wavelength $(\lambda/6)$, although the overall scatterer is 2λ across. The mesh used in this calculation is shown in Fig. 6 and has 475 triangular elements and the apertures are of similar size to the elements. Clearly, it is the geometry which dictates the mesh refinement in this case. In such problems, accurate determination of the near field is important and Fig. 7 shows the near H-field magnitude computed $\lambda/18$ away from the surface for various orders of interpolation due to a plane wave incident normal to the array. Also shown is a reference result based on a fine mesh with 2600 elements. It is clear that the lowest order bases give rise to significant errors and that third-order bases are required to achieve convergence on the coarse mesh. Furthermore, the p-MUS scheme demonstrates a speed-up of ~ 35 over the standard BiCG scheme for this problem.

IV. Conclusion

This paper considers the solution of the EFIE. Hierarchical conforming bases have been developed which are subsequently used in the construction of multilevel Schwarz-type preconditioners. The effectiveness of this approach has been assessed by the computation of scattering from a range of perfectly conducting objects including spheres, cubes, plates, and dihedrals. For problems whose mesh size is determined by the frequency (e.g., RCS of electrically large smooth objects), these schemes require more BPW in order to converge than is demanded by accuracy. As a result the single-level BiCG scheme is generally superior for such cases. For problems where the mesh size is determined by geometry, p-MUS is shown to be faster than conventional schemes by factors of between 5 and 20. It should be noted that these gains are largely independent of any other aspects of the solution (e.g., solver type, other preconditioners, etc.). This work concerns only the use of the EFIE for PEC scatterers and other formulations (MFIE, CFIE) for both PEC and dielectric cases may equally benefit from this hierarchical approach and an assessment of these cases is currently underway.

Appendix
Hierarchical Basis functions

The basis functions used in the paper are listed in Tables I and II and refer to the parent elements shown in Fig 8. Note that $\sigma_{i,j}$

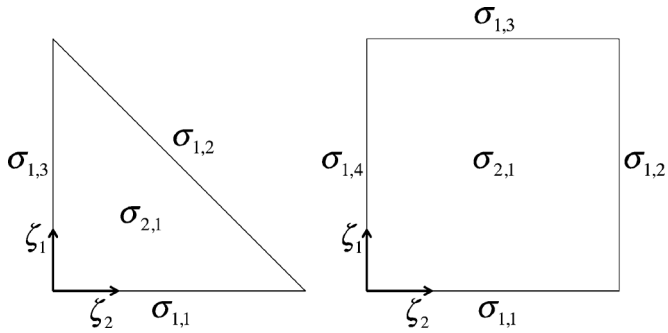

Fig. 8. Parent element and manifold assignments.

denotes the jth $i-$dimensional sub-manifold with which each of the bases are associated, i.e., The second-order edge basis function associated with the third edge of the parent triangle is $\zeta_2 d\zeta_1 + (\zeta_1 + 2\zeta_2 - 1)d\zeta_2$, etc. We have included these due to the fact that there are a number of alternative bases available in the literature, and the precise forms of the bases may have an impact on the performance reported in this paper.

REFERENCES

[1] C.-C. Lu and W. C. Chew, "A multilevel algorithm for solving a boundary integral equation of wave scattering," *Microw. Opt. Technol. Lett.*, vol. 7, no. 10, pp. 466–470, 1994.

[2] J. Lee, J. Zhang, and C.-C. Lu, "Sparse inverse preconditioning of multilevel fast multipole algorithm for hybrid integral equations in electromagnetics," *IEEE Trans. Antennas Propag.*, vol. 52, no. 9, pp. 2277–2287, Sep. 2004.

[3] G. Angiulli, P. Quattrone, and S. Tringali, "An algebraic preconditioner based on properties of the skew-hermitian part of the linear systems arising from the discretization of the e-field integral equation," in *Proc. Int. Conf. Electromagn. Adv. Applicat. (ICEAA '09) 11th Edition*, 2009, pp. 632–635.

[4] P. Rui, R. Chen, Z. Fan, J. Hu, and Z. Nie, "Perturbed incomplete ilu preconditioner for efficient solution of electric field integral equations," *IET Microw. Antennas Propag.*, vol. 1, no. 5, pp. 1059–1063, 2007.

[5] P. Rui, H. Yong, and R. Chen, "Multipreconditioned gmres method for electromagnetic wave scattering problems," *Microw. Opt. Technol. Lett.*, vol. 50, no. 1, pp. 150–152, 2008.

[6] S. M. Rao, D. R. Wilton, and A. W. Glisson, "Electromagnetic scattering by surfaces of arbitrary shape," *IEEE Trans. Antennas Propag.*, vol. AP-30, no. 3, pp. 409–418, May 1982.

[7] W. Cai, T. Yu, H. Wang, and Y. Yu, "High-order mixed RWG basis functions for electromagnetic applications," *IEEE Trans. Microw, Theory Tech.*, vol. 49, no. 7, pp. 1295–1303, Jul. 2001.

[8] M. Ainsworth and J. Coyle, "Hierarchic hp-edge element families for Maxwell's equations on hybrid quadrilateral/triangular meshes," *Comput. Meth. Appl. Mech. Eng.*, vol. 190, no. 49–50, pp. 6709–6703, 2001.

[9] J. P. Webb, "Hierarchal vector basis functions of arbitrary order for triangular and tetrahedral finite elements," *IEEE Trans. Antennas Propag,*, vol. 47, no. 8, pp. 1244–1253, 1999.

[10] L. Andersen and J. Volakis, "Hierarchical tangential vector finite elements for tetrahedra," *IEEE Microw. Guid. Wave Lett.*, vol. 8, no. 3, pp. 127–129, Mar. 1998.

[11] L. Andersen and J. Volakis, "Development and application of a novel class of hierarchical tangential vector finite elements for electromagnetics," *IEEE Trans. Antennas Propag.*, vol. 47, no. 1, pp. 112–120, Jan. 1999.

[12] Z. Ren and N. Ida, "High order differential form-based elements for the computation of electromagnetic field," *IEEE Trans. Magn.*, vol. 36, no. 4, pp. 1472–1478, Jul. 2000, .

[13] M. Ilic and B. Notaros, "Higher order hierarchical curved hexahedral vector finite elements for electromagnetic modeling," *IEEE Trans. Microw. Theory Tech.*, vol. 51, no. 3, pp. 1026–1033, Mar. 2003.

[14] T. Karacolak and E. Topsakal, "Hierarchical mixed-order tangential vector finite elements for tetrahedra," in *Proc. Antennas Propag. Soc. Int. Symp.*, Washington, DC, USA, 2005, vol. 4A, pp. 300–300.

[15] P. Ingelstrom, "A new set of h(curl)-conforming hierarchical basis functions for tetrahedral meshes," *IEEE Trans. Microw. Theory Tech.*, vol. 54, no. 1, pp. 106–114, Jan. 2006.

[16] J. Swartz and D. Davidson, "Curvilinear vector finite elements using a set of hierarchical basis functions," *IEEE Trans. Antennas Propag.*, vol. 55, no. 2, pp. 440–446, Feb. 2007.

[17] P. Ingelstrom, V. Hill, and R. Dyczij-Edlinger, "Comparison of hierarchical basis functions for efficient multilevel solvers," *IET Sci. Meas. Technol.*, vol. 1, no. 1, pp. 48–52, 2007.

[18] J. Lee, "Conforming hierarchical vector elements," in *Proc. Antennas Propag. Soc. Int. Symp.*, San Antonio, TX, USA, 2002, vol. 1, pp. 66–69.

[19] W. Jingguo and J. P. Webb, "Hierarchal vector boundary elements and p-adaption for 3-d electromagnetic scattering," *IEEE Trans. Antennas Propag.*, vol. 45, no. 12, pp. 1869–, Dec. 1997.

[20] D. Ding, R.-S. Chen, Z. Fan, and P. Rui, "A novel hierarchical two-level spectral preconditioning technique for electromagnetic wave scattering," *IEEE Trans. Antennas Propag.*, vol. 56, no. 4, pp. 1122–1132, Apr. 2008.

[21] F. Andriulli, A. Tabacco, and G. Vecchi, "A multiresolution approach to the electric field integral equation in antenna problems," *SIAM J. Sci. Comput.*, vol. 29, no. 1, pp. 1–21, 2007.

[22] M. J. Bluck, A. Hatzipetros, and S. P. Walker, "Applications of differential forms to boundary integral equations," *IEEE Trans. Antennas Propag.*, vol. 54, no. 6, pp. 1781–1796, Jun. 2006.

[23] D. Arnold, R. Falk, and R. Winther, "Finite element exterior calculus, homological techniques, and applications," *Acta Numer.*, vol. 15, pp. 1–155, 2006.

[24] R. Hiptmair, "Finite elements in computational electromagnetism," *Acta Numer.*, vol. 11, pp. 237–, 2002.

[25] E. Jorgensen, J. Volakis, P. Meincke, and O. Breinbjerg, "Higher order hierarchical Legendre basis functions for electromagnetic modeling," *IEEE Trans. Antennas Propag.*, vol. 52, no. 11, pp. 2985–2995, Nov. 2004.

[26] Y. Zhu and A. Cangellaris, "Hierarchical multilevel potential preconditioner for fast finite-element analysis of microwave devices," *IEEE Trans. Microw. Theory Tech.*, vol. 50, no. 8, pp. 1984–1989, Aug. 2002.

[27] M. J. Bluck, "Conforming hierarchical basis functions," *Commun. Comput. Phys.*, vol. 12, no. 4, pp. 1215–1256, Oct. 2012.

Michael Bluck received the B.Sc. degree in mathematics from the University of Kent. Canterbury, U.K., in 1988 and the Ph.D. degree from Imperial College, London, U.K., in 1993, for work on the development of time-domain integral equation methods.

His interests are in the application and development of computational techniques for electromagnetics, nuclear thermal hydraulics, and reactor physics. He is a senior lecturer in the Nuclear Engineering group of the Mechanical Engineering Department, Imperial College, where he is the Deputy Director of the Rolls-Royce Nuclear University Technology Centre.

Nicolas Cinosi graduated as an electronic engineer at the University of Ancona, Ancona, Italy, and received the Ph.D. degree from the University of Bath, Bath, U.K.

His interests focus on the computational analysis of electromagnetic scattering and propagation in optical components. He is currently a Research Associate in the Mechanical Engineering Department, Imperial College, London.

Simon Walker received the B.Eng. and Ph.D. degrees from Imperial College, London, U.K.

His main interests are in the application and development of computational techniques for wave scattering, including finite element and boundary integral equation methods. He is currently a Reader and Head of the Computational Mechanics Group the Mechanical Engineering Department, Imperial College.